

## **ANALYTICAL MODEL FOR PREDICTING THE RESPONSE OF OLD-TYPE COLUMNS REHABILITATED WITH CONCRETE JACKETING UNDER REVERSED CYCLIC LOADING**

**Georgia E. Thermou<sup>1</sup>, Vassilis K. Papanikolaou<sup>1</sup>, and Andreas J. Kappos<sup>1</sup>**

<sup>1</sup> Aristotle University of Thessaloniki  
Thessaloniki 54124, Greece  
gthermou@civil.auth.gr, billy@civil.auth.gr, ajkap@civil.auth.gr

**Keywords:** Reinforced Concrete, Jacket, Retrofit, Strengthening, Shear transfer mechanisms, Cyclic loading.

**Abstract.** *In the study presented herein, an analytical model for predicting the response of members with old-type detailing, rehabilitated with reinforced concrete (R/C) jacketing under reversed cyclic loading is developed. The analytical model considers that there is partial connection between the existing member (core of the retrofitted member) and its outer R/C shell, thus allowing relative slip of the two bodies. Slip takes place at the interface between the existing member and the jacket, mobilizing the shear resistance mechanisms, such as aggregate interlock, friction and dowel action. Constitutive models from the international literature are adopted to describe the mechanisms that resist relative sliding under cyclic shear reversals. Dual-section analysis is adopted to calculate the shear flow at the interface between the existing member and the jacket. An algorithm is developed to estimate the flexural response under cyclic loading taking into account slip at the interfaces. The proposed algorithm is utilized for the derivation of moment – curvature response histories of members tested in the laboratory, selected from a database compiled in the framework of the present study.*

## 1 INTRODUCTION

Reinforced concrete structures hold a significant percentage of the building stock in South Europe and especially in Greece. The vast majority of these structures built in the 70's do not comply with current seismic codes [1]. Due to lack of seismic detailing and capacity design, premature failure is foreseen. Rehabilitation measures are considered necessary and often a combination of both global and local intervention methods provides the most efficient retrofit solution [2]. Reinforced concrete jacketing is an intervention method used extensively in practice to accommodate deficiencies related to global response indices such as stiffness and strength. The use of this method allows uniform distribution of lateral load capacity throughout the structure, thereby avoiding concentrations of lateral load resistance.

Variations of the method are related to the means of connection (i.e. dowels, U-shaped links, etc.) between the 'old' cross section, which serves as the core of the jacketed member, and the jacket itself, along with the preparation of the surface of the existing member (i.e. roughening). All these measures aim to provide full composite action between the two bodies and reduce the effect of slip at the interface between the existing member and the jacket.

The usual practice adopted by intervention codes for proportioning of R/C jacketed members in order to simplify the design procedure is the use of monolithicity factors. These reduction factors are used to obtain the resistance and deformation indices of the jacketed members and are applied to the respective properties of monolithic members with identical geometry. In the case of Eurocode 8, Part 1.3 (§A.4.2, [3]) and under the assumptions of: (i) full composite action between old and new concrete, (ii) application of full axial load in the jacketed member, and (iii) application of the concrete properties of the jacket over the full section of the element, monolithicity factors are equal to  $K_V=0.9$  for shear strength,  $K_{M_y}=1.0$  for moment at yield,  $K_{\theta_u}=1.0$  for the rotation at ultimate, whereas for the rotation at yield, the value  $K_{\theta_y}=1.05$  applies in case that measures for roughening of the interface have been taken and the value  $K_{\theta_y}=1.20$  applies for the rest of the measures taken for the connection of the jacket to the existing member or when no particular measures are taken. The Hellenic code for retrofitting (§8.2.1 5 [4]) suggests monolithicity factors for shear strength  $K_V=0.9$ , for stiffness,  $K_K=0.8$ , and rotation at yield and ultimate  $K_{\theta_y}=1.25$  and  $K_{\theta_u}=0.80$ , respectively.

The values adopted by the codes are empirical, mainly due to the limited understanding of the influence of shear resistance mechanisms mobilized at the interface due to slip. To this purpose an analytical model is developed for predicting the response of R/C jacketed members taking into account slip at the interface between the existing member and the jacket under cyclic loading conditions. The solution algorithm is based on previous research conducted by Thermou *et al.* [5, 6] for monotonic loading. In this paper, it is further modified and extended to account for cyclic shear reversals.

## 2 SHEAR TRANSFER MECHANISMS UNDER CYCLIC LOADING

Shear transfer along interfaces plays a crucial role in the response of composite members. Describing in detail the mechanisms mobilized along interfaces due to slip and their interaction is a rather complex mechanical issue, especially under cyclic loading conditions where degradation should also be accounted for. Although issues of connection between existing and newly cast concrete arise often in retrofitting of R/C structures, as in the case of the R/C jacketing technique, it remains an issue that has not been fully addressed by codes.

Mechanisms that resist sliding (slip) are: (i) aggregate interlock between contact surfaces, including any initial adhesion of the jacket concrete on the substrate; (ii) friction owing to clamping action of reinforcement normal to the interface; and (iii) dowel action of any prop-

erly anchored reinforcement crossing the sliding plane. The first two mechanisms refer to the contribution of concrete, since they are based on the friction resistance of the interfaces. The relationship that describes the contribution of the individual shear transfer mechanisms is:

$$\tau_{tot} = \tau_{agr} + \tau_f + \tau_D = \tau_{agr} + \mu\sigma_N + \tau_D \quad (1)$$

where  $\sigma_N = \sigma_c + p\sigma_s = \nu f_c + \rho\sigma_s$

In the above equation,  $\tau_{agr}$  represents the shear resistance of the aggregate interlock mechanism,  $\mu$  is the interface shear friction coefficient,  $\sigma_N$  is the normal clamping stress acting on the interface and  $\tau_D$  is the shear stress resisted by dowel action in cracked reinforced concrete. The clamping stress represents any normal pressure,  $p$ , externally applied on the interface, but also the clamping action of reinforcement crossing the contact plane as illustrated in Fig. 1 ( $\sigma_s$  is the axial stress of the bars crossing the interface,  $\rho$  is the corresponding reinforcement area ratio,  $\nu = N/(A_c f_c) = \sigma_c / f_c$  is the dimensionless axial load at the interface of  $A_c$  area and  $f_c$  is the concrete compressive strength).

The first two terms in Eq. (1) collectively represent the *contribution of concrete* as they depend on the frictional resistance of the interface planes.

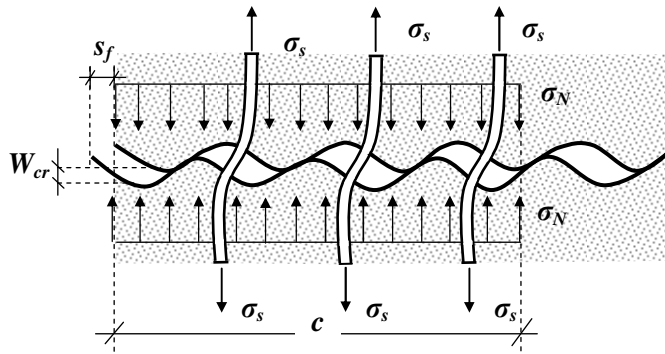


Figure 1: Slip at a concrete interface crossed by reinforcement.

Shear transfer along interfaces has been a subject of ongoing research for many years now. Analytical models and design expressions have been proposed by various researchers, the majority of which are either empirical or based on substantial simplifications. The models found in the literature are classified in two categories. To the first belong those models where all forces are transferred through reinforcement [7-12], whereas the second includes those models that apart from reinforcement contribution include a cohesion term [13-21].

For the needs of the present study, the model of Tassios & Vintzēleou [18], Vintzēleou & Tassios [19, 20] was used because it was the only model found in literature that describes the shear transfer mechanisms under cyclic loading. Furthermore, this model predicted with satisfactory precision the shear resistance developed at the interface between old and new concrete after cross-correlating with the experimental results of a parametric experimental investigation where twenty four (24) specimens of double interface were tested with parameters of study the diameter and the area of reinforcement bars crossing vertically the interface, as well as the degree of interface roughness [22]. The model estimates the combined dowel and shear friction resistances for a given slip value at the interface.

## 2.1 Friction resistance

The shear stress transferred through friction due to slip is described by the following set of equations [18-20]:

$$\frac{\tau(s)}{\tau_{f,u}} = 1.14 \left( \frac{s}{s_u} \right)^{1/3} \quad \text{for } \frac{s}{s_u} \leq 0.5 \quad (2a)$$

$$\frac{\tau(s)}{\tau_u} = 0.81 + 0.19 \left( \frac{s}{s_u} \right) \quad \text{for } \frac{s}{s_u} > 0.5 \quad (2b)$$

where  $s_u$  ( $\approx 2$  mm) is the higher value of slip attained, whereas the higher value of friction resistance,  $\tau_{fu}$ , is equal to:

$$\tau_{fu} = \mu (f_c^2 \sigma_N)^{1/3} \quad (3)$$

where  $\mu$  is the friction coefficient, taken equal to 0.44 for  $s_u=2$ mm.

According to Tassios and Vintzēleou [18], it is assumed that the bars pullout by  $w/2$  from each side of the contact surface and that the separation  $w$  and lateral slip,  $s$ , are related by:  $w=0.6 \cdot s^{2/3}$  (Fig. 1). To calculate the axial stress of the bars crossing the interface,  $\sigma_s$ , the separation  $w$  between contact surfaces as they slide overriding one another is considered (Fig. 1). Considering uniform bond stresses along the embedment length, the axial bar stress,  $\sigma_s$ , at the contact plane is estimated from:

$$\sigma_s = \left( \frac{0.3 s_f^{2/3} E_s f_c}{D_b} \right)^{1/2} \quad (4)$$

where  $E_s$  is the elastic modulus of steel and  $D_b$  is the diameter of the bars clamping the interface (here, the stirrup legs of the jacket).

In case of cyclic loading the frictional resistance is reduced at each cycle according to:

$$\tau_{f,n} = \tau_{f,1} \left\{ 1 - \left[ 0.002(n-1) \frac{f_c}{\sigma_N} \frac{s_f}{s_{f,u}} \right]^{1/3} \right\} \quad (5)$$

where  $\tau_{f,1}$  is the higher frictional resistance value attained in the first cycle. The hysteretic model of frictional resistance is differentiated depending on the value of slip at which reversal takes place. Two cases are identified; in the first, unloading takes place at lower slip values compared to the higher value of slip,  $s < s_u$  (Fig. 2(a), [21]), whereas in the second unloading takes place at the higher value of slip attained,  $s_u$  (Fig. 2(b), [18]).

## 2.2 Dowel resistance

In the model proposed by Vintzēleou & Tassios [19, 20], it is considered that the bar behaves as a horizontally loaded free-headed pile embedded in cohesive soil and that yielding of the dowel and crushing of concrete occur simultaneously. Dowel force,  $F_D$ , is given as a function of slip,  $s$ , by:

$$\frac{F_D(s)}{F_{D,u}} = 0.5 \frac{s}{s_{el}} \quad \text{for } s \leq s_{el} = 0.006 D_b \quad (6a)$$

$$\text{for } \frac{F_D(s)}{F_{D,u}} \geq 0.5 \Rightarrow s = 0.006D_b + 1.76s_u \left[ \left( \frac{F_D(s)}{F_{D,u}} \right)^4 - 0.5 \left( \frac{F_D(s)}{F_{D,u}} \right)^3 \right] \quad (6b)$$

where  $s_{el}$  is the elastic slip value,  $s_u$  is the ultimate slip value,  $F_{D,u}$  is the ultimate dowel force and  $D_b$  is the diameter of the dowels (i.e. the legs of the jacket transverse reinforcement). The ultimate dowel strength and associated interface slip are given by:

$$F_{D,u} = 1.3D_b^2 [f_{cd} f_{yd} (1 - \alpha^2)]^{1/2} = D_b^2 [f_c f_y (1 - \alpha^2)]^{1/2}; \quad s_{D,u} = 0.05D_b \quad (7)$$

where  $\alpha$  is the bar axial stress normalized with respect to its yield value,  $f_{yd}(=f_y/1.15)$  is the design yield strength of steel and  $f_{cd}(=f_{ck}/1.5)$  is the design concrete compressive strength. The dowel resistance constitutive laws are depicted in Fig. 3.

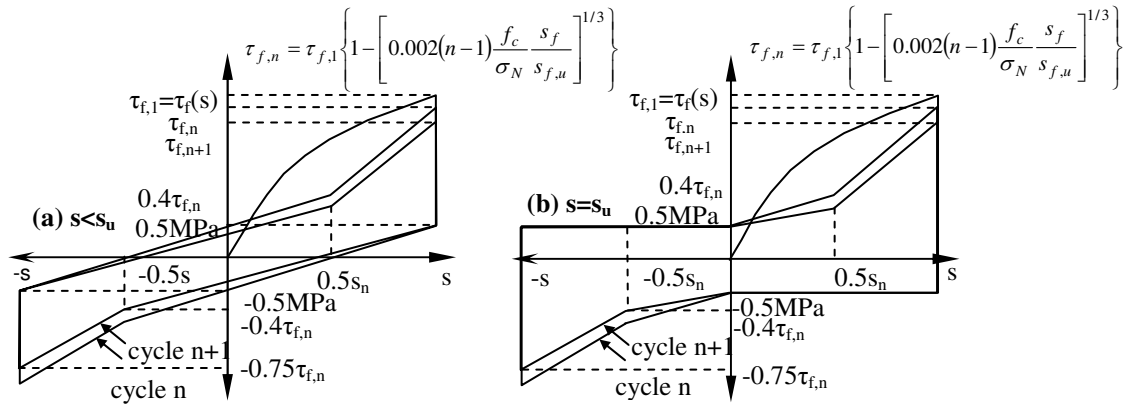


Figure 2: Frictional resistance constitutive laws for (a)  $s < s_u$  [21]; (b)  $s = s_u$  [18].

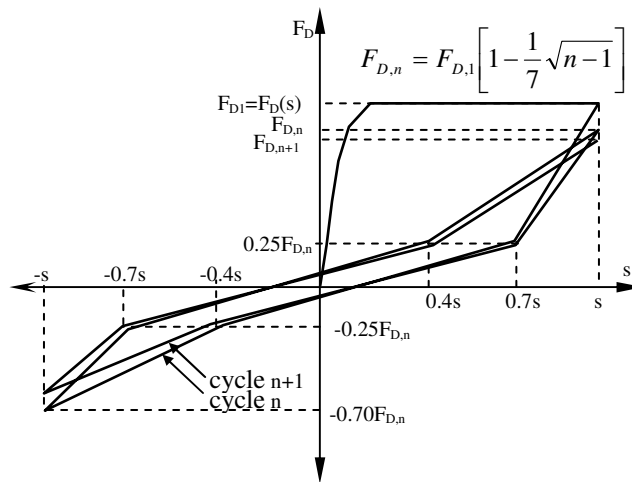


Figure 3: Dowel resistance constitutive law [19, 20].

### 2.3 Interaction of friction and dowel resistance

In case that the bars are subjected simultaneously to tension (pullout due to frictional resistance) and shear (dowel action), then the dowel strength capacity at yield is consumed by both resistance mechanisms. In order to take into account the interaction of the two resistance mechanisms, the higher friction and dowel resistance capacity are determined by the following relationship [21]:

$$\left( \frac{\sigma_s - \sigma_{SN}}{f_{sy}} \right)^{3/2} + \left( \frac{F_D(s)}{F_{D,u}} \right)^{3/2} = 1; \quad \sigma_{SN} = \frac{v \cdot f_c}{\rho + E_c/E_s} \quad (8)$$

where  $\sigma_s$  is the pullout stress mobilized at slip,  $f_c$  is the concrete compressive strength,  $E_c$ ,  $E_s$ , are the elastic modulus of concrete and steel, respectively,  $v(=N/(A_c f_c))$  is the dimensionless axial load, and  $\rho$  is the percentage of reinforcement that crosses the interface.

The solution of Eq. (8) corresponds to a value for  $s_{crit}$ , for which the dowel and friction resistance cannot increase further. This assumption leads to a modification of the hysteretic diagram of dowel action in cyclic loading.

The total shear resistance of an interface with contact area  $A_{int}$  crossed by  $k$  dowels is:

$$F(s) = \tau_f(s)A_{int} + kF_D(s) \quad (9)$$

where  $\tau_f(s)$  and  $F_D(s)$  are calculated from Eqs. (2) and (6), respectively, for a given amount of interface slip.

## 3 ANALYTICAL MODEL OF R/C JACKETED MEMBERS SUBJECTED TO CYCLIC SHEAR REVERSALS

The analytical model for the flexural behaviour of brittle R/C members rehabilitated with concrete jacketing presented herein is based on previous research conducted by Thermou et al. [5, 6] but it is further extended to cyclic loading conditions after a series of adaptations and additions. The proposed analytical model introduces a degree of freedom allowing the relative slip at the interface between the existing member and the jacket. Slip along the member's length is attributed to the difference in normal strains at the contact interfaces (Fig. 4(a)). For flexural analysis, the cross section is divided into three layers which deform with the same curvature,  $\varphi$  (Fig. 4(a)). The two external layers represent the contribution of the jacket, whereas the internal one represents both the core (existing cross section) and the web of the jacket shell. Slip at the interface mobilizes the shear transfer mechanisms such as aggregate interlock, friction owing to clamping action and dowel action of the stirrup legs of the jacket (Fig. 4(b)). The friction and dowel resistance constitutive laws in cyclic loading proposed by Tassios & Vintzēleou [18], Vintzēleou & Tassios [19, 20] are adopted (see section 2) and further modified as described in section 4.2 for the needs of the current study.

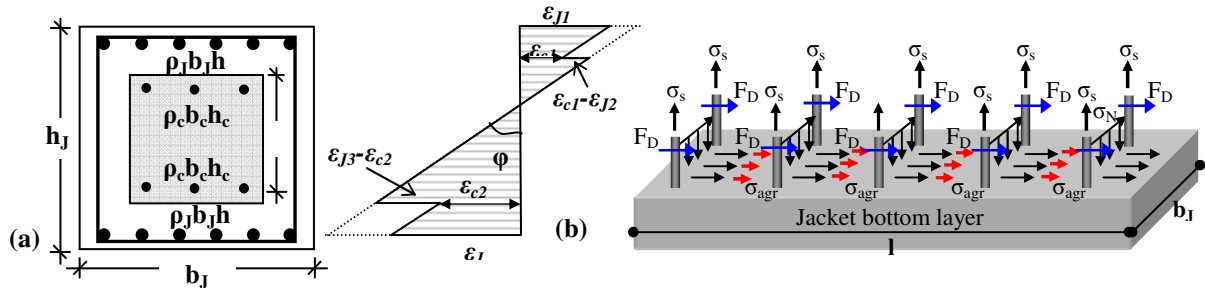


Figure 4: (a) Strain profile of the jacketed cross section; (b) Shear transfer mechanisms at the interface between the jacket and the core.

According to the proposed analytical model of Thermou et al. [5, 6] for R/C jacketed members, shear transfer at the interface between the existing member and the jacket is carried out between half crack intervals along the length of the jacketed member as considered in bond analysis. At the initial stages of loading, cracks form only at the external layers (jacket) increasing in number with increasing load, up to crack stabilization. This occurs when the jacket steel stress at the crack,  $f_{s,cr}$  exceeds the limit [23]:

$$f_{s,cr} > f_{ctm} \frac{1 + \eta \rho_{s,eff}}{\rho_{s,eff}} \quad (10)$$

where  $f_{ctm}$  is the tensile strength of concrete,  $\eta (= E_s/E_{cm})$  is the modular ratio and  $\rho_{s,eff}$  is the effective reinforcement ratio defined as the total steel area divided by the area of mobilized concrete in tension, usually taken as a circular domain with a radius of  $2.5D_b$  around the bar [23]. Using the same considerations in the combined section it may be shown that a number of the external cracks penetrate the second layer (core) of the jacketed member (Fig. 5(a)). The distance between those cracks, taken as  $c$ , is a key element of the proposed methodology.

### 3.1 Crack spacing estimation

After crack stabilization and assuming that the neutral axis depth is about constant in adjacent cross sections, from the free body equilibrium in the tension zone of the core of the composite section (Fig. 5(b)), the crack spacing is defined as follows:

$$c = \frac{0.64 \cdot b_J l_c f_{ct,c}}{n_c D_{b,c} f_{b,c} + n_J D_{b,J} f_{b,J}} \quad (11)$$

where  $b_J$  is the width of the jacketed cross section,  $l_c$  is the height of the tension zone in the core component of the composite cross section,  $f_{ct,c}$  is the tensile strength of concrete core,  $n_c$ ,  $n_J$  are the number of bars in the tension steel layer of the core and the jacket, respectively,  $D_{b,c}$ ,  $D_{b,J}$  are the bar diameter of the core and jacket longitudinal reinforcement, respectively, and  $f_{b,c}$ ,  $f_{b,J}$  are the average bond stress of the core and the jacket reinforcement layer, respectively.

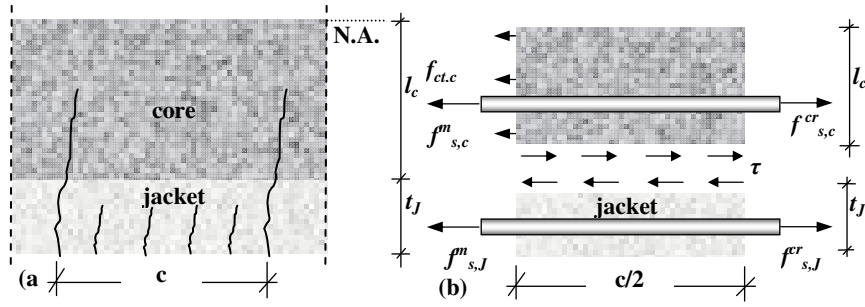


Figure 5: (a) Crack spacing,  $c$ ; (b) Free body equilibrium in the tension zone of the core of the composite section.

### 3.2 Shear stress demand at the interfaces

Shear stress demand at the interfaces,  $\tau_{d,i}$ , is determined by examining the cross section along the height and a member length equal to the distance between successive cracks (Figure 6(a)). The layer force resultant  $\Sigma F_i$  (sum of concrete and steel forces at each layer), for the externally applied axial load,  $N_{ext}$  (considered to be applied to the jacketed section), is used to calculate the vertical shear stress demand of the member,  $\tau_{d,i}$ . With the assumption that the shear flow,  $q$ , reversal takes place at length equal to  $c/2$  (Figure 6(b), where  $c$  is the crack spacing), the average stress demand  $\tau_{d,i}$  is equal to:

$$\tau_{d,i} = \frac{\Sigma F_i}{0.5 c b_j} \quad (12)$$

where  $\Sigma F_i$  is the layer force resultant,  $b_j$  is the width of the jacketed cross section, and  $c$  is the crack spacing length.

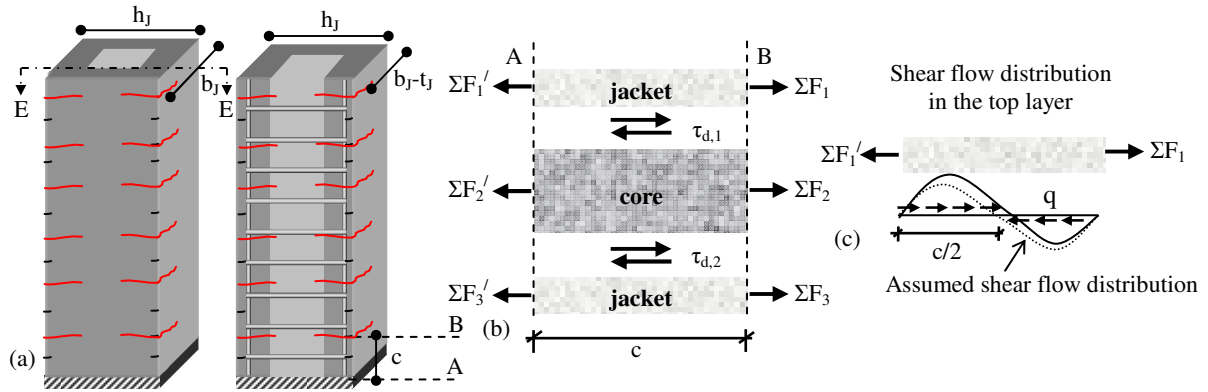


Figure 6: (a) R/C jacketed column; (b) Section equilibrium between adjacent cracks; (c) Assumption for the estimation of shear flow,  $q$ .

## 4 ALGORITHM FOR MOMENT – CURVATURE ANALYSIS

The calculation algorithm aims at the derivation of moment – curvature histories of R/C members retrofitted with R/C jackets taking into account slip at the interfaces between the existing member (core) and the jacket under cyclic loading conditions. Thus, given a curvature loading history (Fig. 7), at each loading step the objective is twofold: (i) equilibrium establishment between the shear stress capacity and demand at the interfaces for relative slip,  $s$ ,



and (ii) establishment simultaneously of force equilibrium at the cross section. Equilibrium is established though an iterative procedure until convergence is achieved.

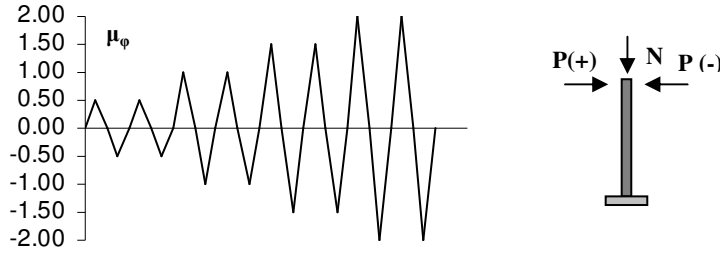


Figure 7: Loading history considered in the calculation algorithm.

In the first step of the analysis (very low curvature value) slip is taken equal to zero at both interfaces. In the next steps, as curvature increases, the inclination of the strain profile is modified (allowing continuously increasing difference of strain at the interfaces) in order to establish cross section equilibrium.

The proposed calculation algorithm comprises the following steps:

For each loading cycle  $\ell$ :

- 1) Set sectional curvature equal to  $\varphi^n(+)$ . Problem unknowns are, the normal strain at the top fiber of the jacketed cross section,  $\varepsilon_{J1}^{n,m}$ , the interface slip at the upper,  $s_1^{n,r}$ , and bottom interfaces,  $s_2^{n,r}$ .
- 2) Estimate the normal strain at the top fiber of the cross section,  $\varepsilon_{J1}^{n,m}$  (Fig. 4(a)).
- 3) Estimate the interface slip at the upper and bottom interfaces,  $s_1^{n,r}$  and  $s_2^{n,r}$ . Slip at the interface is related to the difference of strains at the upper and lower interface,  $\Delta\varepsilon_1^{n,r}$  and  $\Delta\varepsilon_2^{n,r}$ , as follows:

$$s_1^{n,r} = \Delta\varepsilon_1^{n,r} c = (\varepsilon_{c1}^{n,r} - \varepsilon_{j2}^{n,r}) c, \quad s_2^{n,r} = \Delta\varepsilon_2^{n,r} c = (\varepsilon_{j3}^{n,r} - \varepsilon_{c2}^{n,r}) c \quad (13)$$

where variables  $\varepsilon_{c1}^{n,r}$ ,  $\varepsilon_{j2}^{n,r}$  and  $\varepsilon_{j3}^{n,r}$ , and  $\varepsilon_{c2}^{n,r}$  are normal strains in the section layers above and below the contact surfaces (Fig. 4(a)), and  $c$  is the average crack spacing (Eq. (11), Fig. 5(a)).

- 4) Check equilibrium at the interfaces - Shear strength capacity of the top and bottom interface,  $\tau_1^{n,r}$  and  $\tau_2^{n,r}$ , are estimated from the respective slip values,  $s_1^{n,r}$  and  $s_2^{n,r}$ , according to the constitutive laws that describe the behaviour of the interface under cyclic loading (Eqs. 2-9). Shear strength demand at the upper and bottom interface,  $\tau_{d,1}^{n,r}$  and  $\tau_{d,2}^{n,r}$ , are also estimated according to Eq. (12). Check if  $\tau_1^{n,r} = \tau_{d,1}^{n,r}$  and  $\tau_2^{n,r} = \tau_{d,2}^{n,r}$ . If this is valid, then equilibrium is established and the next step follows, otherwise return to step 3 and set  $s_1^{n,r+1} = s_1^{n,r} + ds_1$ ,  $s_2^{n,r+1} = s_2^{n,r} + ds_2$ , where  $ds_i$  is the selected increment in the slip value. Revise slip values at the top and bottom interface till convergence.
- 5) Check cross section equilibrium: The force resultant,  $\Sigma F_i$  (Fig. 6(a)) is calculated at each layer. In case that equilibrium is not established,  $\Sigma \Sigma F_i - N_{ext} \geq \text{tolerance}$ , then the normal strain profile is revised by returning to step 2 and setting  $\varepsilon_{J1}^{n,m+1} = \varepsilon_{J1}^{n,m} + d\varepsilon_J$ , where  $d\varepsilon_J$  is the step increment in the top strain of the jacketed cross section.
- 6) Store the convergent values for which equilibrium at both interface and cross section level was established ( $\varepsilon_{J1}^n = \varepsilon_{J1}^{n,m}$ ,  $s_1^n = s_1^{n,r}$ ,  $s_2^n = s_2^{n,r}$ ).
- 7) Estimate the moment resultant,  $M^n$ .
- 8) Unloading
- 9) Repeat steps 1-7 for  $\varphi^n(-)$

- 10) Unloading
- 11) Repeat steps 1-10 for  $\ell=\ell+1$ . Calculations stop when the shear capacity of the interface is exhausted.

An original program was developed based on the proposed solution algorithm as described in the flowchart of Fig. 8. Fiber analysis was considered. The behaviour of concrete and steel was described by adopting uniaxial constitutive laws under cyclic loading from the literature (details are provided in section 4.1). The constitutive laws for the description of the shear transfer mechanisms mobilized due to slip at the interface are based on the models of Tassios & Vintzēleou [18], Vintzēleou & Tassios [19, 20], further enhanced to account for arbitrary loading history (load cycles of unequal amplitude).

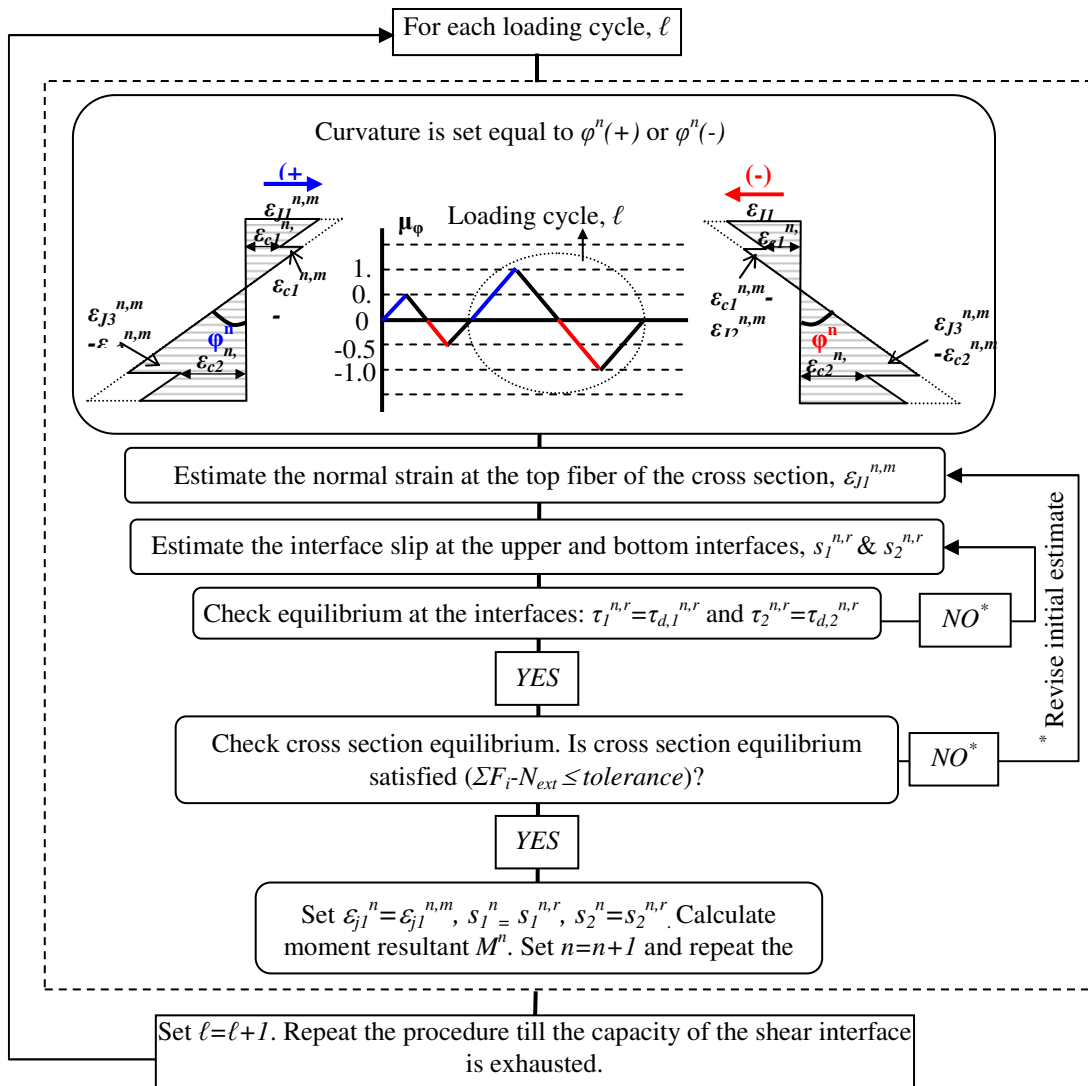


Figure 8: Flowchart of the proposed algorithm.

#### 4.1 Material constitutive laws

**Concrete:** The constitutive law for concrete adopted is based on the model of Mander et al. [24] as far as the relationship between stresses-strains is concerned and on the hysteresis rules of Martinez-Rueda & Elnashai [25]. Confinement due to transverse reinforcement (taken into

account by factor  $K$ ) is considered constant during loading and follows the relationships proposed by Mander et al. [24]. This law is adequate for modelling R/C elements, especially those subjected to random cyclic loading (e.g. seismic loading). The general shape of the response curve is presented in Fig. 9(a).

**Steel:** The constitutive law for steel utilized in the proposed algorithm is based on the stress-strain relationship developed by Menegotto-Pinto [26] in combination with the rules of isotropic hardening proposed by Fillippou et al. [27]. It is suitable for modelling reinforced concrete elements subjected to cyclic loading as in seismic conditions. The response curve in its general form is presented in Fig. 9(b).

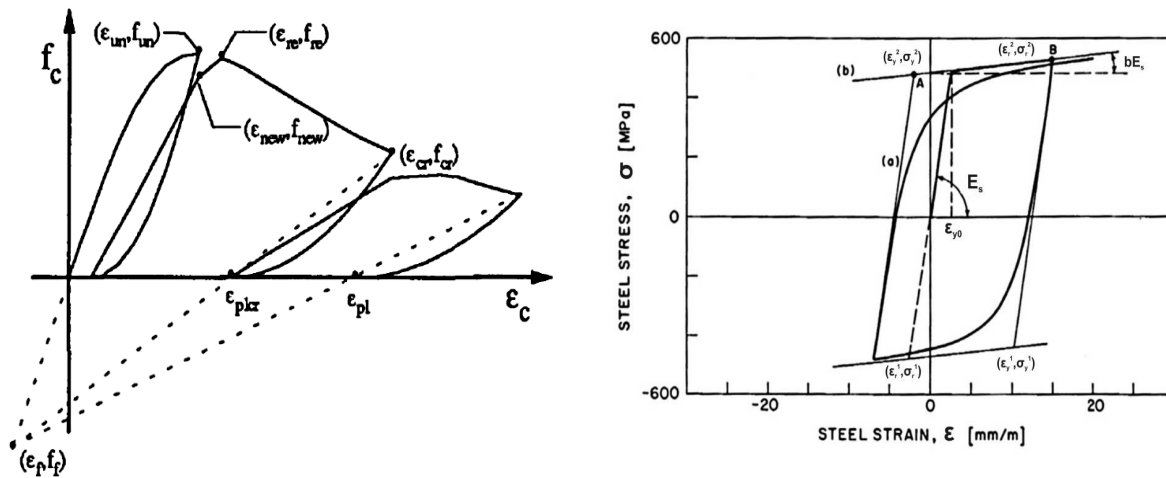


Figure 9: (a) Concrete [25]; (b) Steel constitutive laws [27].

## 4.2 Interface shear resistance constitutive law

The friction and dowel resistance models as proposed by Tassios & Vintzēleou [18], Vintzēleou and Tassios [19, 20] were further modified to account for the case of non-symmetric reversed cyclic loading. In Fig. 10, for a given random loading history that depends on slip magnitude,  $s$ , the extracted dowel resistance hysteretic curve and the total resistance curve according to Eq. (9) are shown.

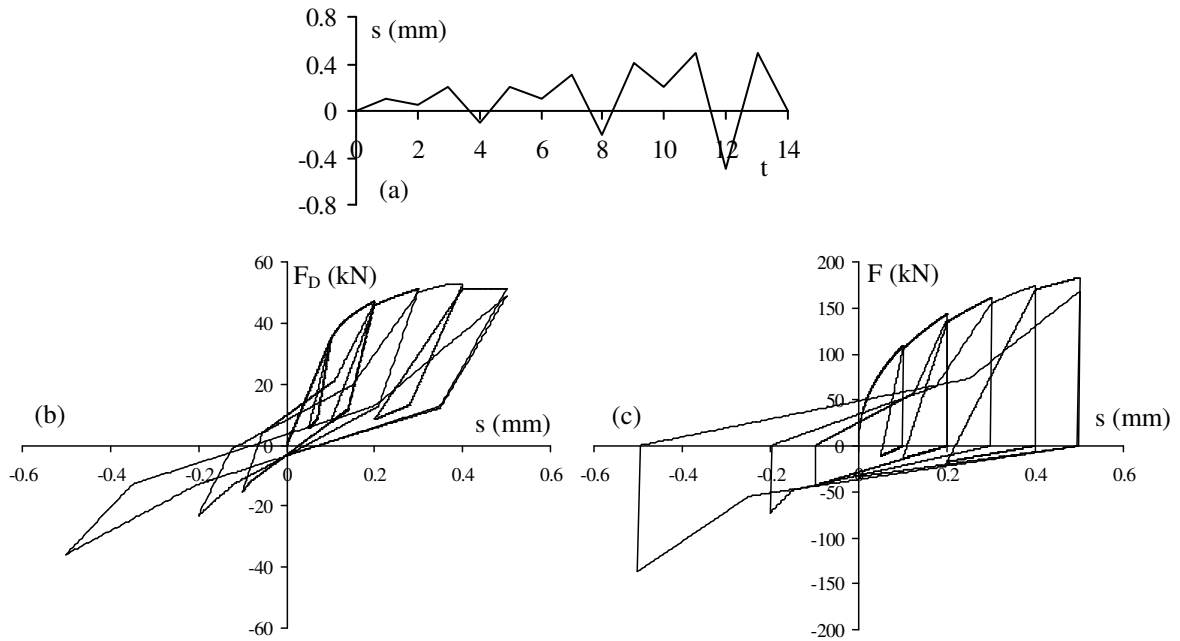


Figure 10: (a) Non-symmetric loading history; (b) Dowel resistance hysteretic curve; (c) Total interface resistance hysteretic curve.

## 5 RESULTS OF THE ANALYSIS

In this section the proposed analytical model is used for estimating the flexural response of R/C jacketed members for the case that slip at the interface between the jacket and the existing member is neglected. The case-studies selected to be presented herein were taken from the experimental database which was created for the needs of this ongoing study.

### 5.1 Presentation of the experimental database

An experimental database was created which includes forty four (44) specimens from eleven (11) experimental studies. The database includes specimens where various connection measures were taken between the existing member and the jacket, whereas the jacket construction was done using shotcrete or cast-in-place concrete. The range of database parameters is shown in Table 1. The database along with the symbols used are presented in detail in Tables A1 and A2 of the Appendix.

The specimens selected to be analyzed with the proposed algorithm are specimens R2R [29] and Q-RCR [36]. Details on the geometrical and material characteristics are presented in Tables A1 and A2 of the Appendix.

Existing cross section		Jacket	
$b_c$ (mm)	200~350	$b_J$ (mm)	260~550
$h_c$ (mm)	200~500	$h_J$ (mm)	260~650
$D_{b,c}$ (mm)	10~20	$D_{b,J}$ (mm)	10~20
$\rho_{lc}$ (%)	0.81~2.05	$\rho_{lJ}$ (%)	0.75~1.64
$D_{bs,c}$ (mm)	6~8	$D_{bs,J}$ (mm)	6~10
$s_c$ (mm)	50~265	$s_J$ (mm)	50~100
$\rho_{wc}$ (%)	0.16~0.66	$\rho_{wJ}$ (%)	0.22~0.94
$f_c$ (MPa)	22.9~58.2	$f_c$ (MPa)	7~68.7
$f_y$ (MPa)	313~550	$f_y$ (MPa)	400~520
$f_{yw}$ (MPa)	350~520	$f_{yw}$ (MPa)	330~599
$L_s/h_c$	3.2~11.7	$L_s/h_J$	2.5~7.0
Μάτιση ( $D_b$ )	15~45	$L_s$ (mm)	1000~3500
		$v$ (%)	0~26

Table 1: Range of database parameters.

## 5.2 Results of the case studies considered

Specimens P2R [29] and Q-RCR [36] are subjected to the applied curvature ductility history presented in Fig. 11. Each loading cycle increases by  $\frac{1}{4}$  of  $\varphi_y$ . The curvature at yield,  $\varphi_y$ , was estimated by the following simplified expression [4]:

$$\varphi_y = 1.77 \frac{f_y}{E_s h_J} \quad (1)$$

where  $f_y$  is the yield strength of steel of the reinforcement bars of the jacket,  $h_J$  the height of the jacketed member and  $E_s$  the modulus of elasticity of steel. For specimen P2R curvature at yield is  $\varphi_y=1.6 \times 10^{-2}$  (rad/m), displacement at yield is  $\Delta_y=5.5$  mm and drift at yield is  $\theta_y=0.54\%$ , whereas for specimen Q-RCR curvature at yield is  $\varphi_y=1.08 \times 10^{-2}$  (rad/m), displacement at yield  $\Delta_y=9.2$  mm and drift at yield  $\theta_y=0.57\%$ . The hysteretic response of the two test specimens is depicted in Figures 12 and 13.

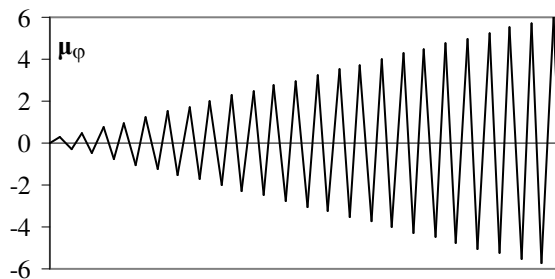


Figure 11: Curvature loading history subjected to specimens P2R [29] and Q-RCR [36].

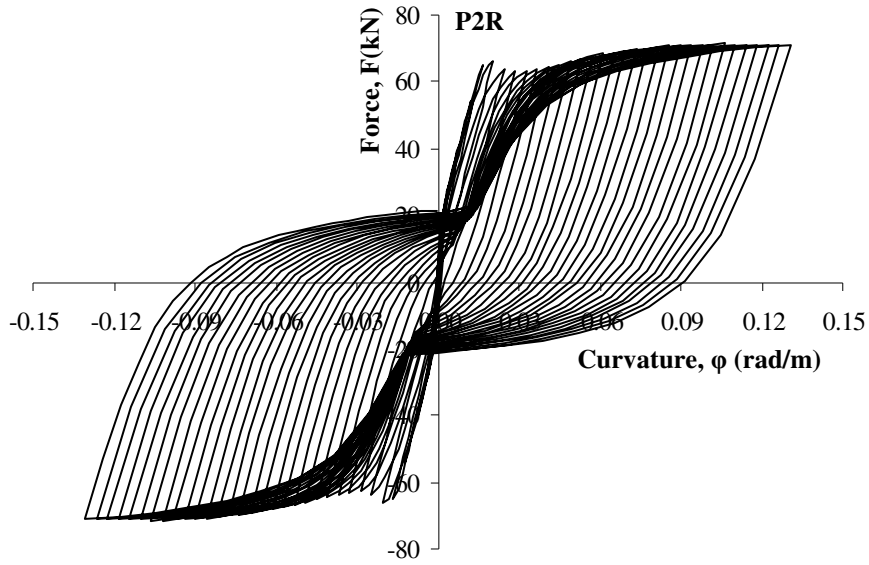


Figure 12: Response of specimen P2R [29] to cyclic loading conditions for the case that slip is neglected.

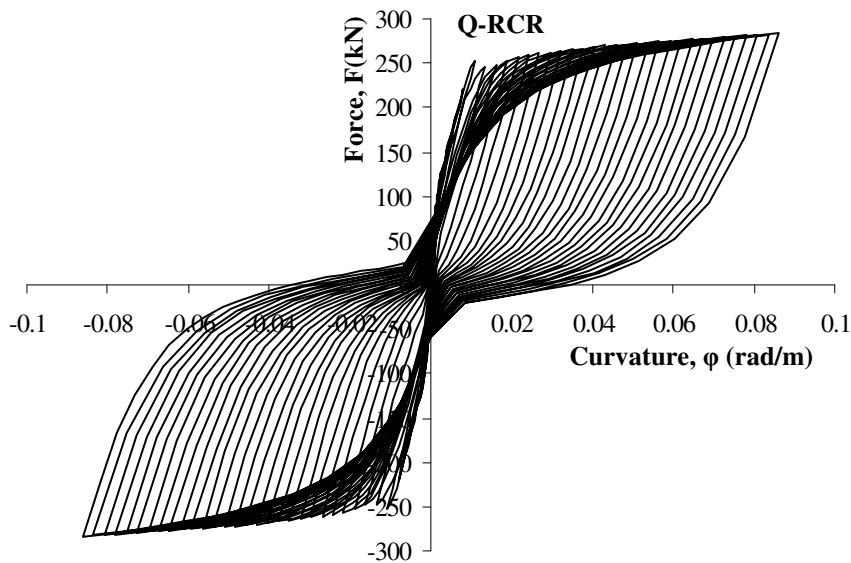


Figure 13: Response of specimen Q-RCR [36] to cyclic loading conditions for the case that slip is neglected.

## 6 CONCLUSIONS

An analytical model for predicting the response of old-type columns rehabilitated with concrete jacketing under reversed cyclic loading was developed. The composite cross section is divided into three layers which develop the same curvature. The proposed analytical model allows slip at the interface between the existing member and the jacket. Shear transfer mecha-

nisms are mobilized due to sliding at the interface between existing and new concrete. The shear capacity is described by constitutive models for cyclic loading conditions and is given as a function of slip. The shear demand at the interface is controlled by the flexural stresses on the cross section and by the spacing of cracks in the longitudinal direction. Equilibrium at the interfaces is established when shear capacity and demand are equalized. An algorithm was developed for determining the moment – curvature histories of R/C jacketed members with partial connection between the existing member (core) and the jacket. The response of test specimens selected from a database compiled within the framework of this work was studied by utilizing the proposed solution algorithm for null slip at the interface.

## ACKNOWLEDGEMENTS

The research conducted in this paper was funded by the Hellenic Earthquake Planning and Protection Organization (E.P.P.O.); the authors gratefully acknowledge this support.

## REFERENCES

- [1] Eurocode 8, Design of structures for earthquake resistance - Part 1: general rules, seismic actions and rules for buildings. EN1998-1-2004:E, European Committee for Standardization (CEN), Brussels, 2004.
- [2] G. E Thermou, A. S. Elnashai, Seismic retrofit schemes for R/C structures and local-global consequences. *Journal of Progress in Structural Engineering and Materials*, Wiley InterScience, **8**(1), 1-15, 2006
- [3] Eurocode 8, Design of structures for earthquake resistance - Part 3: Assessment and retrofitting of buildings. EN 1998-3:2005(E), European Committee for Standardization (CEN), Brussels, 2005.
- [4] KANEPE, Interventions Code (of Greece). Earthquake Planning and Protection Organization (E.P.P.O.), Final draft, Sep. 2010 (in Greek).
- [5] G.E. Thermou, S.J. Pantazopoulou, A.S. Elnashai, Design and assessment models and spectra for repaired reinforced concrete structures. Mid-America Earthquake Center Report, CD release 09-01, 2009.
- [6] G.E. Thermou, S.J. Pantazopoulou, A.S. Elnashai, Flexural behaviour of brittle R/C members rehabilitated with concrete jacketing. *Journal of Structural Engineering*, *ASCE*, **133**(10), 1373-1384, 2007.
- [7] ACI Committee 318, Building Code Requirements for Reinforced Concrete (ACI 318-95) and Commentary ACI 318 R-95. *American Concrete Institute*, Detroit, 16-1 -16-10, 1995.
- [8] ACI Committee 318, Building Code Requirements for Reinforced Concrete (ACI 318-99) and Commentary ACI 318 R-99. *American Concrete Institute*, Detroit, 133 – 142, 1999.
- [9] ACI Committee 318, Building Code Requirements for Reinforced Concrete (ACI 318-02) and Commentary ACI 318 R-02. *American Concrete Institute*, Detroit, 139–154, 2002.

- [10] P.W., Birkeland, H.W. Birkeland, Connections in precast concrete construction. *Journal of American Concrete Institute*, **63**(3), 345-368, 1966.
- [11] J.C. Walraven, Fundamental analysis of aggregate interlock. *Structural Division, ASCE*, **107**, No. ST11, 2245-2270, 1981.
- [12] E.R. Loov, K.A. Patnaik, Horizontal shear strength of composite concrete beams with a rough interface. *PCI Journal*, 48-69, 1994.
- [13] J.C.T.S. Climaco, P.E. Regan, Evaluation of bond strength between old and new concrete in structural repairs. *Magazine of Concrete Research*, **53**(6), 377-390, 2001.
- [14] H.A. Mattock, M.N. Hawkins, Shear transfer in reinforced concrete- recent research. *PCI Journal*, 55-75, 1972.
- [15] H.A. Mattock, K.W. Li, C.T. Wang, Shear transfer in lightweight reinforced concrete. *PCI Journal*, 20-39, 1976.
- [16] H.A. Mattock, Shear friction and high-strength concrete. *Structural Journal, ACI*, **98**(1), 50-59, 2001.
- [17] F.J. Vecchio, M.P. Collins, The modified compression-field theory for reinforced concrete elements subjected to shear. *ACI Journal*, **83**(2), 219-581, 1986.
- [18] T. Tassios, V.E. Vintzēleou, Concrete-to-concrete friction. *ASCE J. Struct. Eng.*, **113**(4), 832-849, 1987.
- [19] E. Vintzēleou, T. Tassios, Mathematical models for dowel action under monotonic and cyclic conditions. *Magaz. of Concrete Research*, **38**(134), 13-22, 1986.
- [20] E. Vintzēleou, T. Tassios, Behaviour of dowels under cyclic deformations. *ACI Struct. J.*, **84**(1), 18-30, 1987.
- [21] I. Vassilopoulou, P. Tassios. Shear transfer capacity along a R/C. crack under cyclic sliding. *Proc., fib Symposium*, Technical Chamber of Greece), Athens, Greece, Paper No. 271., 2003.
- [22] O. Dimitriadou, V. Kotsoglou, G.E. Thermou, A. Savva, S.J. Pantazopoulou, Experimental study of concrete interfaces in sliding shear. Technical Chronicles, *Journal of the Technical Chamber of Greece (TCG)*, **25**(2-3), 123-136 (in Greek), 2005.
- [23] *fib Model Code 2010*, First complete draft - Vol. 2, Bull. 56, Lausanne, Apr. 2010.
- [24] J.B. Mander, M.J.N. Priestley, R. Park, Theoretical stress-strain model for confined concrete. *Journal of Structural Engineering*, **114**(8), 1804-1826, 1988.
- [25] J.E. Martinez-Rueda, A.S. Elnashai, Confined concrete model under cyclic load. *Materials and Structures*, **30**(197), 139-147, 1997.
- [26] M. Menegotto, P.E Pinto, Method of analysis for cyclically loaded R/C plane frames including changes in geometry and nonelastic behaviour of elements under combined normal force and bending. *Proc. IABSE Symposium*, Lisbon, Portugal, 1973.
- [27] F.C Filippou., E.P Popov, V.V. Bertero, Effects of bond deterioration on hysteretic behaviour of reinforced concrete joints. *Report No. UCB/EERC-83/19*, University of California, Berkeley, 1983.
- [28] M. Rodriguez, R. Park, Seismic load tests on reinforced concrete columns strengthened by jacketing. *ACI Struct. J.*, **91**(2), 150-159, 1994.



- [29] A.M. Gomes, J. Appleton, Repair and strengthening of R.C. elements under cyclic loading. *Proc., 11<sup>th</sup> Europ. Conf. Earthq. Eng.*, A.A. Balkema (Rotterdam, The Netherlands), Paris, France, CD-ROM, 1998.
- [30] A. Ilki, K. Darilmaz, I Bakan, M. Zorbozan, E. Yuksel, S. Haruhan, F. Karadogan, Jacketing of Prefabricated Columns. *Proc.2nd Japan-Turkey Workshop on Earthquake Engineering*, Istanbul, Turkey, 329-336, 1998.
- [31] K.G. Vadoros, S.E. Dritsos, Interface treatment in shotcrete jacketing of reinforced concrete columns to improve seismic performance. *J. Struct. Eng. and Mech.*, **23**(1), 43-61, 2006a.
- [32] K.G. Vadoros, S.E. Dritsos, Axial preloading effects when reinforced concrete columns are strengthened by concrete. *Progress in Struct. Eng. and Mat. J.*, **8**(3), 79-92, 2006b.
- [33] K.G. Vadoros, S.E. Dritsos, Concrete jacket construction detail effectiveness when strengthening R/C columns. *Construction and Building Materials*, **22**, 264-276, 2008.
- [34] E.N.B.S. Júlio, F.A.B. Branco, V.D Silva, Reinforced Concrete Jacketing—Interface Influence on Monotonic Loading Response. *ACI Structural Journal*, 102(2), 252-257, 2005.
- [35] S. Bousias, A.-L Spathis, M.N Fardis, Concrete or FRP jacketing of columns with lap splices for seismic rehabilitation. *Journal of Advanced Concrete Technology*, **4**(3), 431-444, 2006.
- [36] S. Bousias, D. Biskinis, M. Fardis, A. Spathis, Strength, stiffness, and cyclic deformation capacity of the concrete jacketed members. *ACI Struct. J.*, **104**(5), 521-531, 2007a.
- [37] S. Bousias, A.-L Spathis, M.N Fardis, Seismic retrofitting of columns with lap-spliced smooth bars through FRP or Concrete Jackets. *Journal of Earthquake Engineering*, **11**, 653-674, 2007b.
- [38] E.N.B.S. Júlio, F.A.B. Branco, Reinforced Concrete Jacketing—Interface Influence on Cyclic Loading Response. *ACI Structural Journal*, **105**(4), 471-477, 2008.

## APPENDIX

### Symbols used in the database:

- $b_c$ ;  $b_j$ : width of the existing and the jacketed cross section;
- $D_{b,c}$ ;  $D_{b,j}$ : bar diameter of the core and the jacket longitudinal reinforcement, respectively;
- $D_{bs,c}$ ;  $D_{bs,j}$ : bar diameter of the stirrups of the core and the jacket, respectively;
- $d_c$ ;  $d_j$ : depth of the existing and the jacketed cross section, respectively;
- $f_{c,c}$ ;  $f_{c,j}$ : core and jacket concrete cylinder uniaxial compressive strength, respectively;
- $f_{y,c}$ ;  $f_{y,j}$ : yield strength of the longitudinal reinforcement of the core and jacket, respectively;
- $f_{yw,c}$ ;  $f_{yw,j}$ : yield strength of the transverse reinforcement of the core and jacket, respectively;
- $h_c$ ;  $h_j$ : height of the existing and the jacketed cross section, respectively;
- $L_s$ : shear span length;
- $n_{c,mid}$ ;  $n_{j,mid}$ : total number of web longitudinal reinforcement bars of the core and the jacket, respectively;
- $n_c$ ;  $n_j$ : total number of top and bottom longitudinal reinforcement bars of the core and the jacket, respectively;

$s_c$ ;  $s_J$ : stirrup distance in the existing and jacketed cross section respectively;

Greek symbols:

$v$ : dimensionless axial load % estimated based on the compressive strength of the jacket concrete quality.

$\rho_{lc}$ : longitudinal reinforcement ratio of the existing cross section defined as  $A_{sc,tot}/(b_c h_c)$ , where  $A_{sc,tot}=(n_c+n_{c,mid})D_{b,c}^2/4$

$\rho_{lJ}$ : longitudinal reinforcement ratio of the jacketed cross section defined as  $A_{sJ,tot}/(b_J h_J - b_c h_c)$ , where  $A_{sJ,tot}=(n_J+n_{J,mid})D_{b,J}^2/4$

$\rho_{wc}$ ;  $\rho_{wJ}$ : volumetric ratio of stirrups of the existing and the jacketed cross section, respectively.

Table A1: Database – Details of original test specimens.

Reference	No	Existing specimens													Lap splice length ( $D_b$ )			
		$b^*$	$b^*$	$d^*$	$n_c$	$n_{cmid}$	$D_{bc}^*$	$p_{lc}^{\#}$	Strut legs	$D_{bsc}^*$	$s_c^*$	$p_{wc}^{\#}$	$f_{cs}^*$	Bar type		$f_{ys}^*$	$f_{ywc}^*$	$L_s/h_c$
Rodríguez & Park (1994)	1	SS1	350	350	295	6	2	20	2.05	4	6	265	0.16	29.5	pl	325	350	4.1
	2	SS2	350	350	295	6	2	20	2.05	4	6	265	0.16	29.5	pl	325	350	4.1
	3	SS3	350	350	295	6	2	20	2.05	4	6	265	0.16	29.5	pl	325	350	4.1
	4	SS4	350	350	295	6	2	20	2.05	4	6	265	0.16	25.9	pl	325	350	4.1
Gomes & Appleton (1998)	5	P2R	200	200	173	4	0	12	1.13	2	6	150	0.22	53.2	def	480	480	5.0
	6	P3R	200	200	173	4	0	12	1.13	2	6	50	0.66	58.2	def	480	480	5.0
	7	P4	200	200	173	4	0	12	1.13	2	6	150	0.22	56.2	def	480	480	5.0
Ilki et al. (1998)	8	7	300	300	269	6	2	16	1.79	2	8	100	0.38	50.6	def	550	425	11.7
	9	8	300	300	269	6	2	16	1.79	2	8	100	0.38	47.1	def	531	425	11.7
	10	9	300	300	269	6	2	16	1.79	2	8	100	0.38	44.3	def	531	425	11.7
Vandoros and Dritsos (2006a, 2006b, 2008)	11	M	250	250	225	4	0	14	0.98	2	8	200	0.24	24.7	pl	313	425	6.4
	12	W	250	250	225	4	0	14	0.98	2	8	200	0.24	22.9	pl	313	425	6.4
	13	D	250	250	225	4	0	14	0.98	2	8	200	0.24	27	pl	313	425	6.4
	14	R	250	250	225	4	0	14	0.98	2	8	200	0.24	27	pl	313	425	6.4
	15	RD	250	250	225	4	0	14	0.98	2	8	200	0.24	27	pl	313	425	6.4
	16	N	250	250	225	4	0	14	0.98	2	8	200	0.24	27	pl	313	425	6.4
	17	NP	250	250	225	4	0	14	0.98	2	8	200	0.24	23.8	pl	313	425	6.4
18	E	250	250	225	4	0	14	0.98	2	8	200	0.24	36.8	pl	313	425	6.4	
Júlio et al. (2005)	19	M2	200	200	180	6	0	10	1.18	2	6	150	0.22	28.9	def	400	400	5.0
	20	M3	200	200	180	6	0	10	1.18	2	6	150	0.22	28.4	def	400	400	5.0
	21	M4	200	200	180	6	0	10	1.18	2	6	150	0.22	28.3	def	400	400	5.0
	22	M5	200	200	180	6	0	10	1.18	2	6	150	0.22	28.4	def	400	400	5.0
	23	M6	200	200	180	6	0	10	1.18	2	6	150	0.22	28.7	def	400	400	5.0
	24	M7	200	200	180	6	0	10	1.18	2	6	150	0.22	28.8	def	400	400	5.0

Table A1 (cont.): Database – Details of original test specimens.

Reference	No	Specimens	Existing specimens													Lap splice length ( $D_b$ )			
			$b^*$	$b^*$	$d^*$	$n_c$	$n_{c,mid}$	$D_{b,c}^*$	$\rho_{lc}^{\#}$	Stirrup legs	$D_{b,s,c}^*$	$s_c^*$	$\rho_{w,c}^{\#}$	$f_{c,s}^{\#}$	Bar type		$f_{y,s}^{\#}$	$f_{y,w,s}^{\#}$	$L_s/h_c$
Bousias et al. (2006)	25	R-RCL1	250	500	470	4	0	18	0.81	2	8	200	0.24	36.7	def	514	425	3.2	15
	26	R-RCL3	250	500	470	4	0	18	0.81	2	8	200	0.24	36.8	def	514	425	3.2	30
	27	R-RCL4	250	500	470	4	0	18	0.81	2	8	200	0.24	36.3	def	514	425	3.2	45
Bousias et al. (2007a)	28	Q-RCW	250	250	220	4	0	14	0.98	2	8	200	0.24	22.9	pl	313	425	6.4	-
	29	Q-RCD	250	250	220	4	0	14	0.98	2	8	200	0.24	27.4	pl	313	425	6.4	-
	30	Q-RCR	250	250	220	4	0	14	0.98	2	8	200	0.24	27.7	pl	313	425	6.4	-
Bousias et al. (2007b)	31	Q-RCRD	250	250	220	4	0	14	0.98	2	8	200	0.24	26.3	pl	313	425	6.4	-
	32	Q-RC	250	250	220	4	0	14	0.98	2	8	200	0.24	26.3	pl	313	425	6.4	-
	33	Q-RCM	-	-	-	-	-	-	-	-	-	-	-	-	-	-	-	-	-
Bousias et al. (2007b)	34	Q-RCpd*	250	250	220	4	0	14	0.98	2	8	200	0.24	23.1	pl	313	425	6.4	-
	35	Q-RCL1	250	250	220	4	0	14	0.98	2	8	200	0.24	27.5	pl	313	425	6.4	15
	36	Q-RCL2	250	250	220	4	0	14	0.98	2	8	200	0.24	25.6	pl	313	425	6.4	25
	37	Q-RCL01pd	250	250	220	4	0	14	0.98	2	8	200	0.24	28.1	pl	313	425	6.4	15
	38	Q-RCL02pd	250	250	220	4	0	14	0.98	2	8	200	0.24	28.1	pl	313	425	6.4	25
Júlio and Branco (2008)	39	M2	200	200	180	6	0	10	1.18	2	6	150	0.22	28.9	def	520	520	5.0	-
	40	M3	200	200	180	6	0	10	1.18	2	6	150	0.22	28.6	def	520	520	5.0	-
	41	M4	200	200	180	6	0	10	1.18	2	6	150	0.22	28.5	def	520	520	5.0	-
	42	M5	200	200	180	6	0	10	1.18	2	6	150	0.22	28.6	def	520	520	5.0	-
	43	M6	200	200	180	6	0	10	1.18	2	6	150	0.22	28.7	def	520	520	5.0	-
	44	M7	200	200	180	6	0	10	1.18	2	6	150	0.22	28.9	def	520	520	5.0	-

\* mm, # %, \$ MPa, Lap splice length ( $D_b$ ): given as a function of the bar diameter of long. reinforcement ( $D_b$ ), Bar type: pl - plain bars, def - ribbed bars

Table A2: Database – Details of retrofitted test specimens.

Reference	No	Specimen	Retrofitted specimens												Pre-damaged	Loading	Connection measure	Jacket type	Anchorage of long. reinf.						
			$b_j^*$	$h_j^*$	$d_j^*$	$n_j$	$n_{jmid}$	$D_{b,j}^*$	$\rho_{b,j}$	$\rho_{u,j}$	Strut legs	$D_{bs,j}^*$	$s_j^*$	$\rho_{w,j}^{\#}$						$f_{c,j}^{\#}$	Bar type	$f_{y,j}^{\#}$	$f_{w,y,j}^{\#}$	$I_s/h_j$	$V^{\#}$
Rodríguez & Park (1994)	1	SS1	550	550	512	8	0	16	0.89	2	10	95	0.36	32.9	def	502	340	2.6	10	1425	✓	c	R	C	HS
	2	SS2	550	550	512	8	0	16	0.89	2	10	95	0.36	34	def	502	340	2.6	10	1425	-	c	R	C	HS
	3	SS3	550	550	503	8	4	12	0.75	4	10	72	0.94	19.4	def	491	330	2.6	10	1425	-	c	R	C	HS
	4	SS4	550	550	503	8	4	12	0.75	4	10	72	0.94	25.2	def	491	330	2.6	10	1425	✓	c	R	C	HS
Gomes & Appleton (1998)	5	P2R	260	260	233	4	0	12	1.64	2	6	75	0.33	58.2	def	480	480	3.8	6	1000	✓	c	RE	C	E
	6	P3R	260	260	233	4	0	12	1.64	2	6	50	0.49	49.6	def	480	480	3.8	7.1	1000	✓	c	RE	C	E
	7	P4	260	260	233	4	0	12	1.64	2	6	75	0.33	56.2	def	480	480	3.8	6.3	1000	M	c	-	-	-
		8	7	500	500	470	10	6	14	1.54	2	8	100	0.22	14.9	def	501	425	7.0	0	3500	✓	m	R	C
Ilki et al. (1998)	9	8	500	500	470	10	6	14	1.54	2	8	100	0.22	7	def	501	425	7.0	0	3500	✓	c	R	C	E
	10	9	500	500	470	10	6	14	1.54	2	8	100	0.22	12.9	def	501	425	7.0	0	3500	✓	c	R	C	E
Vandoros and Dritsos (2006a, 2006b, 2008)	11	M	400	400	360	4	0	20	1.29	2	10	100	0.44	24.7	def	487	599	4.0	23	1600	-	c	-	C	AF
	12	W	400	400	360	4	0	20	1.29	2	10	100	0.44	18.8	def	487	599	4.0	24	1600	-	c	W	C	AF
	13	D	400	400	360	4	0	20	1.29	2	10	100	0.44	55.8	def	487	599	4.0	9	1600	-	c	D	S	AF
	14	R	400	400	360	4	0	20	1.29	2	10	100	0.44	55.8	def	487	599	4.0	9	1600	-	c	R	S	AF
	15	RD	400	400	360	4	0	20	1.29	2	10	100	0.44	55.8	def	487	599	4.0	9	1600	-	c	RD	S	AF
	16	N	400	400	360	4	0	20	1.29	2	10	100	0.44	17.8	def	487	599	4.0	26	1600	-	c	W's	C	AF
	17	NP	400	400	360	4	0	20	1.29	2	10	100	0.44	34.5	def	487	599	4.0	14	1600	-	c	W'sP	C	AF
18	E	400	400	360	4	0	20	1.29	2	10	100	0.44	24	def	487	599	4.0	24	1600	-	c	DW's	C	AF	
Júlio et al. (2005)	19	M2	270	270	250	6	0	10	1.43	2	6	75	0.31	68.6	def	400	400	3.7	3.4	1000	-	m	GL	C	E
	20	M3	270	270	250	6	0	10	1.43	2	6	75	0.31	28.4	def	400	400	3.7	8.2	1000	M	m	-	C	E
	21	M4	270	270	250	6	0	10	1.43	2	6	75	0.31	64.8	def	400	400	3.7	3.6	1000	-	m	NS	C	E
	22	M5	270	270	250	6	0	10	1.43	2	6	75	0.31	67.8	def	400	400	3.7	3.4	1000	-	m	R	C	E
	23	M6	270	270	250	6	0	10	1.43	2	6	75	0.31	66.7	def	400	400	3.7	3.5	1000	-	m	RD	C	E
	24	M7	270	270	250	6	0	10	1.43	2	6	75	0.31	65.5	def	400	400	3.7	3.6	1000	-	m	RP	C	E

Table A2 (cont.): Database – Details of retrofitted test specimens.

Reference	No	Specimen	Retrofitted specimens													Pre-damaged	Loading	Connection measure	Jacket type	Anchorage of long. reinf.					
			$b_j^*$	$h_j^*$	$d_j^*$	$n_j$	$n_{jmid}^*$	$D_{bj}^*$	$P_{uj}^{\#}$	Stirrup legs	$D_{bsj}^*$	$s_j^*$	$P_{vj}^{\#}$	$f_{cs}^*$	Bar type						$f_{ys}^*$	$f_{ywj}^*$	$I_s/h_j$	$V^{\#}$	$I_s^*$
Bousias et al. (2006)	25	R-RCL1	400	650	600	6	0	18	1.13	2	10	100	0.44	55.3	def	514	599	2.5	6.6	1600	-	c	NS	S	AF
	26	R-RCL3	400	650	605	6	0	18	1.13	2	10	100	0.44	55.3	def	514	599	2.5	6.6	1600	-	c	NS	S	AF
	27	R-RCL4	400	650	600	6	0	18	1.13	2	10	100	0.44	55.3	def	514	599	2.5	5.2	1600	-	c	NS	S	AF
Bousias et al. (2007a)	28	Q-RCW	400	400	355	4	0	20	1.29	2	10	100	0.45	28.7	def	487	599	4.0	13	1600	-	c	W	S	AF
	29	Q-RCD	400	400	355	4	0	20	1.29	2	10	100	0.45	55.3	def	487	599	4.0	8.5	1600	-	c	D	S	AF
	30	Q-RCR	400	400	355	4	0	20	1.29	2	10	100	0.45	55.3	def	487	599	4.0	9	1600	-	c	R	S	AF
	31	Q-RCRD	400	400	355	4	0	20	1.29	2	10	100	0.45	53.2	def	487	599	4.0	9.4	1600	-	c	RD	S	AF
	32	Q-RC	400	400	355	4	0	20	1.29	2	10	100	0.45	55.3	def	487	599	4.0	8	1600	-	c	-	S	AF
33	Q-RCM	400	400	350	4	0	20	1.29	2	10	100	0.45	30.6	def	487	599	4.0	18	1600	M	c	-	S	AF	
Bousias et al. (2007b)	34	Q-RCpd	400	400	355	4	0	20	1.29	2	10	100	0.45	24.1	def	487	599	4.0	8	1600	✓	c	-	C	AF
	35	Q-RCL1	400	400	360	4	0	20	1.29	2	10	100	0.44	55.3	def	487	599	4.0	8.5	1600	-	c	-	S	AF
	36	Q-RCL2	400	400	360	4	0	20	1.29	2	10	100	0.44	55.3	def	487	599	4.0	8.5	1600	-	c	-	S	AF
	37	Q-RCL01pd	400	400	360	4	0	20	1.29	2	10	100	0.44	28.7	def	487	599	4.0	16	1600	✓	c	R	S	AF
	38	Q-RCL02pd	400	400	360	4	0	20	1.29	2	10	100	0.44	28.7	def	487	599	4.0	17.5	1600	✓	c	R	S	AF
Júlio and Branco (2008)	39	M2	270	270	250	6	0	10	1.43	2	6	75	0.31	68.7	def	520	520	3.7	3.4	1000	-	c	GL	C	E
	40	M3	270	270	250	6	0	10	1.43	2	6	75	0.31	28.6	def	520	520	3.7	8.2	1000	M	c	-	C	E
	41	M4	270	270	250	6	0	10	1.43	2	6	75	0.31	63.3	def	520	520	3.7	3.7	1000	-	c	NS	C	E
	42	M5	270	270	250	6	0	10	1.43	2	6	75	0.31	61	def	520	520	3.7	3.8	1000	-	c	R	C	E
	43	M6	270	270	250	6	0	10	1.43	2	6	75	0.31	65	def	520	520	3.7	3.6	1000	-	c	RD	C	E
	44	M7	270	270	250	6	0	10	1.43	2	6	75	0.31	65.9	def	520	520	3.7	3.5	1000	-	c	RP	C	E

\* mm, # %, § MPa, Lap splice length ( $D_b$ ): given as a function of the bar diameter of the longitudinal reinforcement ( $D_b$ ), Bar type: pl - plain bars, def - ribbed bars, Pre-damaged: M - monolithic construction, Loading: c - cyclic, m - monotonic, Connection measures: NS - natural surface, W - welding between the longitudinal reinforcement of the existing cross section and that of the jacket via U-shaped links, D - dowels, R - roughening of the full lateral surface of the old column, RD - dowels and roughening, RE - roughening and epoxy application on the existing column, GL - greased layer placed on the existing column, RP - roughening and jacket construction when the axial load was applied, Ws: welding of stirrup ends of the first four stirrups from the base of the jacketed member, WSP: welding of stirrup ends of the first four stirrups from the base of the jacketed member, Jacket construction: C - cast in place, S - shotcrete, Anchorage of longitudinal reinforcement of the jacket: AF - embedment of the reinforcement when the original column was cast, E: anchorage of the reinforcement to the footing in predrilled holes with an epoxy resin.